Proceedings of ASME Turbo Expo 2022
Turbomachinery Technical Conference and Exposition
GT2022
June 13-17, 2022, Rotterdam, The Netherlands

GT2022-81988

DIRECT NUMERICAL SIMULATIONS OF AERODYNAMIC PERFORMANCE OF WIND TURBINE AIRFOIL BY CONSIDERING FLAP-WISE BLADE OSCILLATIONS

Mahdi Erfanian Nakhchi Toosi[1], Mohammad Rahmati[1]

[1]Faculty of Engineering and Environment, Northumbria University, Newcastle upon Tyne, NE1 8ST, UK

ABSTRACT

Aeroelasticity of modern wind turbines is a critical issue which can significantly affect the structural integrity and lifetime of the wind turbine blades. However, previous aeroelastic or aerodynamic studies were mostly concentrated on low-fidelity numerical methods, and the details of flow separation and vortex generation over wind turbine airfoils cannot be detected with these methods. In this study, a high-fidelity direct numerical model is used to investigate the details of flow separations and laminar separation bubbles (LSB) over a NACA-0012 wind turbine airfoil under oscillation. The simulations are conducted at Reynolds number of Re=1.3×10^5 and the blade has harmonic pitch-wise oscillations at Mach number of $Ma_\infty = 0.4$. *Strong fluctuations are observed in the wake region of the vibrating wind turbine blade. The results show that the blade vibrations have a significant influence on vortex generation and separation point over wind turbine blades. details of flow structure over wind turbine blades compared to previously proposed models*.

Keywords: Wind turbine airfoil; Flow separation; Blade vibrations; Lift coefficient; Direct numerical simulation.

1. INTRODUCTION

The wind power production farms, as a reliable source of renewable energy, have been attracting major interest to reduce greenhouse gas emissions. The wind turbines currently operating worldwide provide only 5% of the global electricity need [1] but this is expected to increase significantly over the next few years. The focus on offshore wind energy industry has been more on maximising the power generation, and less on assessing and minimizing aeroelastic effects. In complex wind farm layouts in the UK, the wind turbines are becoming larger and taller these days. The largest offshore windfarm in North Sea will produce electricity for 4.5 million households, while the horizontal-axis turbine blades are more than 100 meters long.

However, using bigger offshore wind turbines brings many new challenges to the wind farm designers. One of the most important challenges, is aeroelastic vibrations of long turbine blades. These oscillations and flexibility have significant influence on the flow structure aerodynamic performance of a wind turbine [2]. Moreover, these blades oscillations have influence on the noise generation of the wind farm layouts [3].

Several low-fidelity computational fluid dynamics (CFD) analysis such as Reynolds average Navier-Stokes (RANS) models have been widely utilized in the past years to investigate the flow behavior and aerodynamic characteristics of the wind turbines by considering the blades vibrations. But these low-fidelity methods are unable to detect the instantaneous features of vortex generation, flow disturbance and instabilities in the wake region of the turbine blades. These vorticities have significant influence on the performance of the wind turbines. Therefore, it is vital to perform high-fidelity CFD simulations to precisely analyze the flow structure and predict the flow separation point and dynamic stall by considering the blade vibrations of horizontal-axis wind turbines (HAWTs). However, such details have not been investigated yet. Therefore, it is essential to perform a high-fidelity numerical analysis over wind turbine blades by considering the blades aeroelastic vibrations under realistic physical conditions at different Reynolds numbers.

Several numerical and experimental studies have been conducted over various wind turbine airfoils at wide range of design parameters [4-6]. Koca et al. [7] experimentally studied the vorticities and laminar separation bubble (LSB) formation over NACA-4412 airfoil at different Re numbers and angle of attack (AoA). The experiments were performed using hot-film technique for visualization of turbulent flow streamlines over the airfoil. Their results revealed that LSB size becomes smaller by decreasing the AoA. Zhang et al. [8] tried to modify the shape of NACA-0018 airfoil to improve the efficiency of vertical-axis wind turbines. Their numerical analysis showed that The NACA airfoils with a pitch angle of 6^o, perform better than the other modified thickness cases. The results revealed that the separating point on the suction side of the airfoils appears faster on the thinner airfoils than the thicker ones. In the numerical study of Saleem and Kim [9] tip clearance effects on the aerodynamic characteristics of NACA-9415 airfoil were investigated. They

deduced that the blade tip gaps could improve the turbine power generation at specific wind speeds.

Açıkel and Genç [10] investigated the flow structure and LSB over NACA-4412 aerofoil at low Reynolds numbers. The experiments revealed that LSB formation can be delayed by using partially flexible membrane as a passive flow control technique. Furthermore, the lift force was enhanced by using the newly proposed control strategy, while drag force was decreased. Wahidi et al. [11], experimentally investigated the flow structure and LSB formation over NACA-4412 airfoil. They concluded that AoA has noticeable influence on detachment and reattachment on the surface of the blade. Besides, pairs of forward and backward vorticities were created in the separated areas. These vorticities have significant impact on the flow disturbance and velocity fluctuations in the separated region. Arabgolarcheh et al. [12] employed the actuator line method (ALM) to investigate the aerodynamic performance of the floating offshore wind turbines. O'meara and Mueller [13] experimentally studied the LSB formation on NACA 663-018 aerofoil at $5\times10^4 < \mathrm{Re} < 2\times10^5$, and $(8^\circ < AoA < 12^\circ)$. The experiments showed that LSB thickness was diminished by increasing the Reynolds number. Additionally, raising the AoA can increase LSB thickness over the NACA airfoil.

Precise prediction of flow separation point, and details of vortex generation and instantaneous pressure fluctuations play an important role in the design of turbine blades. Therefore, it is essential to perform high-fidelity numerical analysis to predict these characteristics over blade airfoils at different AoAs and Reynolds numbers. Alam and Sandham [14] conducted a numerical analysis on LSB formation and transition onset over a turbine airfoil. The simulations showed that the flow transition is occurred due to the Kelvin–Helmholtz instabilities in the separated shear-layer. Zhang et al. [15] performed a numerical study to investigate the effects of winglet vortex generator on the power output improvement of the vertical-axis wind turbines. The simulations revealed that the tip-vortex variations due to the winglet vortex generators have noticeable impact on the flow separation and vortex generation over the surface of the blades.

The spectral-hp element method is one of the newly developed high-fidelity numerical methods in aerodynamic analysis of turbulent incompressible and compressible flows. This direct numerical method is based on transient analysis to capture the details of flow separation and instantaneous vortex generation over the turbine blades [16]. Moreover, this method provides the ability to add aeroelastic vibrations to the geometry using a mapping function or a moving reference frame. This DNS method hugely decreases the computation time requirement compared to the other available high-fidelity methods, which makes it suitable for complex flow simulations by considering all important physical parameters. This method is based on an open-source code named NEKTAR++, and it is developed at Imperial College London. This numerical method is developed by Sherwin and Ainsworth [17] to investigate the unsteady flow structure and vorticities in the separated region of the airfoils. The functions of this approach is recently extended by Moxey et al. [18] to improve the numerical model with more advanced convergence control techniques to make it possible to perform DNS at wide range of inflow velocities and vibration frequencies. Cassinelli et al. [19] used spectral-hp element method to investigate the flow separation and vorticity generation over a turbine blade. The results revealed that the proposed model can accurately predict the pressure coefficient on the surface of the blade at $\mathrm{Re}=1.6\times10^5$ and the results are in good agreement with experimental data.

One of the most popular active flow control techniques of the wind turbines is the blades vibrations [20]. The fluid remains more attached to the blade surface due to the oscillations. Nevertheless, the flow separation is strongly dependent to the inflow velocity and the angle of attack (AoA). In the numerical study of Lei et al. [21], the effects of active vibrations of E387 aerofoil on the flow structure were investigated at Re=30,000. They concluded that proposing a high-fidelity numerical model is essential to accurately detect the instantaneous laminar separation bubble formation over the blades. The main limitation of using high-fidelity models is huge computational recourses required compared to time-averaged turbulent models such as RANS models. The results revealed that the separation point can be controlled at different AoAs, while the lift coefficient was increased without noticeable increment in unfavorable drag coefficient. Munday and Jacob [22] experimentally investigated the effects of vibrations on the flow structure and LSB over NACA-4415 airfoil at different camber sizes. The experiments showed that the flow detachment and reattachment points significantly depend on the inflow velocity and AoAs. In the numerical work of Khatam et al. [23], the authors examined the flow separation over a NACA-4415 airfoil at low Reynolds numbers. The simulations showed the oscillations could considerably diminish the separated region over the suction side of the blade. The details of the earlier research done on oscillating airfoils are summarized in Table 1.

TABLE 1. SUMMARY OF THE PREVIOUS STUDIES DONE ON OSCILLATING AIRFOILS.

Author	Study	Method	Re [10^6]	Airfoil	Oscillations
Carr et al. [24]	Expr.	-	1.3-3.5	NACA0012	Pitch-wise
McCroskey et al. [25]	Expr.	-	4	NACA0012	Pitch-wise
Piziali [26]	Expr.	-	2	NACA0015	Pitch-wise
Ekaterinaris [27]	Numr.	2D-RANS	2-4	NACA0012, 0015	Pitch-wise
Raffel et al. [28]	Expr.	-	0.373	NACA0012	Pitch-wise
Ramsay et al. [29]	Expr.	-	0.75-1.4	S809 Airfoil	Pitch-wise
Barakos & Drikakis [30]	Numr.	2D-RANS	1-4.6	NACA0012, 0015	Pitch-wise
Lee & Gerontakos [31]	Expr.	-	1.35	NACA0012	Pitch-wise
Amandolese [32]	Expr.	-	10	NACA63-421	Pitch-wise
Wang et al. [33]	Numr.	2D-RANS	1.35-3.73	NACA0012	Pitch-wise

Lei et al. [21]	Numr.	2D-URANS	0.3	NACA0012	Pitch-wise
Kim and Xie [34]	Numr.	2D-LES	1.35	NACA0012	Pitch-wise
Gharali and Johnson [35]	Numr.	2D-RANS	1.35	NACA0012	Pitch-wise
Zhu et al. [36]	Numr.	3D-URANS	8.67	NREL S809	Pitch-wise
Jokar et al. [37]	Numr.	Modal study	-	NREL WT	Flap-wise

Based on the above literature review, wind turbine blades oscillations have significant impact on the flow structure, and vortex generation over the airfoil surfaces. Previous studies over oscillating airfoils are mostly experimental or low-fidelity two-dimensional analysis. However, the details of complex flow disturbance and separation point on the suction side of the blade cannot be detected with low-fidelity models. Therefore, it is essential to perform a three-dimensional high-fidelity numerical analysis to detect instantaneous pressure fluctuations, LSB formation, and transition onset at different realistic physical conditions. Besides, previous studies over oscillating airfoils were mostly focused on pitching oscillations. But flap-wise vibrations have huge impact on the flow structure over the wind turbine blades. Consequently, performing a high-fidelity DNS can help wind turbines blade manufacturers to better understand the physical reasons of flow separation, vortex generation, lift and drag coefficient over wind turbine blades by considering the aeroelastic oscillations. In this study, a novel high-fidelity numerical analysis based on the spectral-hp element method is conducted to investigate the effects of flap-wise oscillations on the aerodynamic characteristics of NACA-0012 airfoil at different AoAs and inflow velocities. The proposed model can precisely detect the instantaneous LSB formation over the surface of the blades, pressure coefficient, flow detachment and reattachment at various inflow conditions. In addition, the proposed DNS model, requires much smaller computation resources compared to the other DNS/LES models, which is a key parameter in complex numerical analysis.

2. PHYSICAL DESCRIPTION

The schematic view of a horizontal-axis wind turbine with NACA-0012 airfoil with a chord length (C) of 0.25 m at the mid-section (L_z=0.2-0.3) is shown in Figure 1. The angle of attack is selected in the range of ($0^o < \alpha < 20^o$) in this study. The inlet velocity is uniform and the Reynolds number ($Re = U_{in}C/\nu$) is in the range of 50,000 to 135,000 at low Mach numbers (Ma=0.4). The air density is 1.2 kg/m^3, and viscosity (μ) is 1.789×10^{-5} kg/(m.s). The Cartesian coordinate system (x, y, z) is selected to describe the flow directions. The blade is made of composite materials, approximated by the orthotropic material properties, which is utilized in new wind turbines to reduce weight. The physical properties of the blades material which are popular in the design of light-weight wind turbine blades can be found in Ref. [38]. The first natural frequency of the NACA-4412 wind turbine blade section is selected as f=0.64Hz which is identical to the DTU 10MW wind turbine natural frequency. The vibration amplitude in the flap-wise direction is set as A=1% of the chord length, which is in good agreement with the oscillation amplitude of the large horizontal-axis wind turbines.

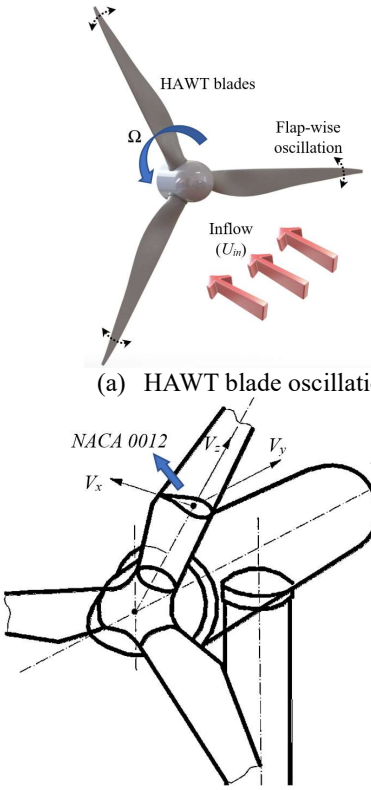

(a) HAWT blade oscillations

(b) Wind turbine mid-section airfoil

FIGURE 1: SCHEMATIC VIEW OF THE OSCILLATING WIND TURBINE AIRFOIL AND PHYSICAL PARAMETERS.

3. MATHEMATICAL MODEL

The three-dimensional incompressible Navier-Stokes equations for simulating the air flow over the turbine blade are expressed as:

$$\partial_t \mathbf{u} + (\mathbf{u}.\nabla)\mathbf{u} = -\nabla p + \nu\nabla^2\mathbf{u} \quad (1)$$

$$\nabla.\mathbf{u} = 0 \quad (2)$$

where $\mathbf{u}$ is the air velocity tensor, p is the pressure, and $\nu = \frac{\mu}{\rho}$ is the kinematic viscosity of the working fluid.

The Spectral-hp element method used in this DNS study, uses a two-dimensional mesh, and expands it in the span direction by using Fast Fourier Transform. This method significantly improves reduce the computation time, which is essential for complex turbulent flow simulations at high Reynolds numbers. The spectral-hp element method is written in an open-source code named NEKTAR++. This code is developed at Imperial College London as a powerful code for modelling various incompressible and compressible flows with and without aeroelastic vibrations. The latest master version of this code is used for this study on ARCHER-2 HPC with 16 dual AMD Rome CPU nodes at 2.2GHz with total 2048 cores. The

details of the aerodynamic forces over the oscillating NACA airfoil are provided in Figure 2.

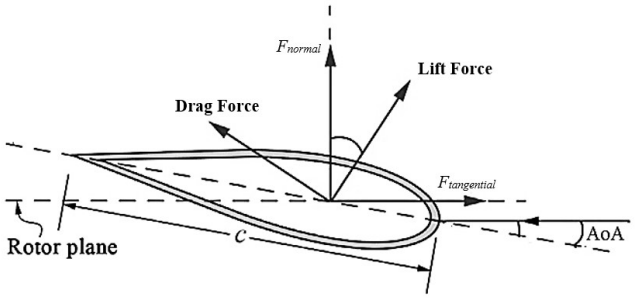

FIGURE 2: NACA 0012 DESIGN PARAMETERS AND FORCES.

3.1. Spectral-hp element method

To use the spectral-hp element method, the local mesh must firstly decompose into a mapped region using modal/nodal expansions through a mapping function imposed in the solver. With the mapping function, it is possible to impose time-dependent oscillations on the airfoil blade with specific vibration frequencies. It is possible to choose continuous Galerkin (CG) and discontinuous Galerkin (DG) schemes for the computations [39]. In this research, continuous Galerkin (CG) method is chosen for the DNS simulations over oscillating NACA-0012 airfoil, which helps convergency of the simulations at higher Reynolds numbers. Based on the Galerkin scheme, the momentum equation can be expressed as:

$$\partial_t \mathbf{u} = N(\mathbf{u}) - \nabla p + \nu \boldsymbol{L}(\mathbf{u}) \tag{3}$$

where $N(\mathbf{u}) = -(\mathbf{u}.\nabla)\mathbf{u}$ and $L(\mathbf{u}) = \nu\nabla^2\mathbf{u}$ are the nonlinear convective and viscous terms, respectively. This equation can be discretized with backward differentiation expression. After discretization of the convective term with polynomial extrapolation, the Navier-Stokes equation at a time step $(\Delta t = n + 1)$ will be expressed as:

$$\frac{\lambda_0 u^{n+1} - \sum_{m=0}^{J_i-1} \alpha_m u^{n-m}}{\Delta t} = \sum_{m=0}^{J_e-1} \beta_m N\,(u^{n-m}) - \nabla p^{n+1} + \nu L(u^{n+1}) \tag{4}$$

where α, β and λ are the equation factors, and J_e and J_i are the combination of the explicit and implicit terms. The Equation (4) can be simplified as:

$$\frac{\lambda_0 u^{n+1} - u^*}{\Delta t} = N^* - \nabla p^{n+1} + \nu L(u^{n+1}) \tag{5}$$

where $u^* = \sum_{m=0}^{J_i-1} \alpha_m u^{n-m}$ and $N^* = \sum_{m=0}^{J_e-1} \beta_m N\,(u^{n-m})$ are simplified expressions in the Galerkin scheme. By performing integration over the total computation domain $\Omega = \bigcup_{e\in\varepsilon} \Omega_e$, where Ω_e are the sub elements in the physical domain [40]:

$$\int_\Omega \nabla p^{n+1}.\nabla\phi d\Omega = \int_\Omega \left(\frac{u^* - \gamma_0 \bar{u}^{n+1}}{\Delta t} + N^* - \nu(\nabla \times \nabla \times u)^+ \right).\nabla\phi d\Omega \tag{6}$$

In which $\nabla\phi$ is the flow stream function. The details of the solving algorithm are presented in Figure 3. It can be seen that the aim is to compute the Advection, Poisson, and Helmholtz terms in the governing equations. The mapping function is used for imposing the oscillations to the airfoil wall. More details of the computation strategy in spectral-hp element method can be found in the recent study of Nakhchi et al. [4].

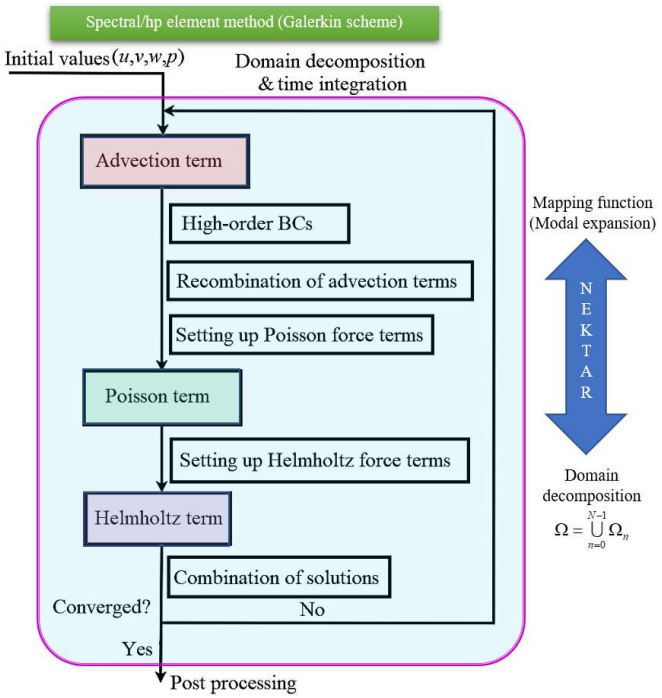

FIGURE 3: SOLUTION FLOWCHART OF DNS STUDY WITH SPECTRAL-HP ELEMENT METHOD.

The details of the mesh generation and domain configuration are provided in Figure 4. For better description of the mesh, the grid is shown for P=5. It means that each tetrahedral element is divided into four sections on each side. The inflow is uniform, and high-order outflow boundary condition is imposed at the outlet to ensure convergency and accuracy of the numerical results. Periodic boundary condition is imposed on the upper and lower walls of the domain. Tetrahedral mesh is used for the flow domain and prism boundary-layer mesh with 8 layers with the minimum size of 0.003 m for the first layer with the growth rate of 1.15 is employed near the blade surface to capture flow separation, and turbulent vorticities in the near-wall regions. A refined mesh is used in the wake region for better visualization of instantaneous vorticity generation in this region. The following equation is employed to compute the high-order outflow pressure:

$$p^{n+1} = \nu \mathbf{n}.\nabla.\mathbf{u}^{*,n+1}.\mathbf{n} - \frac{1}{2}|\mathbf{u}^{*,n+1}|^2 S_0(\mathbf{n}.\mathbf{u}^{*,n+1}) + f_b^{n+1}.\mathbf{n} \tag{7}$$

where $S_0(n.\mathbf{u}) = \frac{1}{2}(1 - \tanh\frac{n.\mathbf{u}}{u_f \delta})$ is a step function, u_f is the characteristics velocity, and δ is a dimensionless constant [41]. The velocity vectors at the high-order outflow can be computed by:

$$\nabla \mathbf{u}^{n+1}.\mathbf{n} = \frac{1}{\nu}\Big[p^{n+1}\mathbf{n} + \frac{1}{2}|\mathbf{u}^{*,n+1}|^2 S_0(\mathbf{n}.\mathbf{u}^{*,n+1}) - \nu(\nabla.\mathbf{u}^{*,n+1})\mathbf{n} - f_b^{n+1}\Big] \quad (8)$$

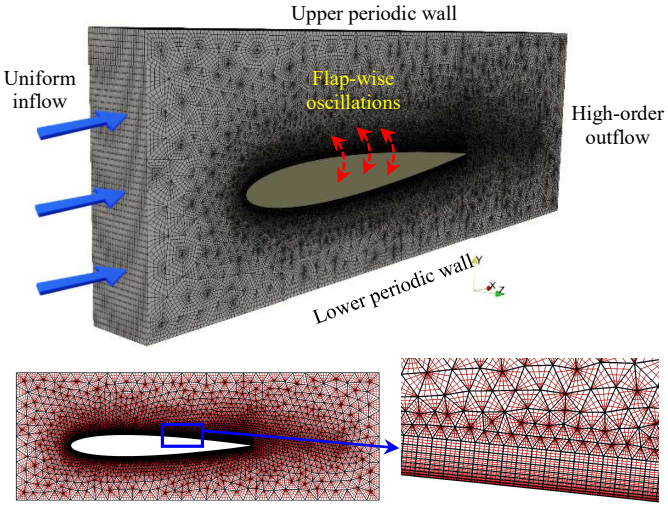

FIGURE 4: DETAILS OF MESH GENERATION AND INFLATED BOUNDARY LAYER.

3.2. Grid study

One of the key parts of the CFD simulations over the wind turbine airfoil, is to find the most appropriate mesh size to achieve the most accurate results without significant increment in the computation times. One of the most important parameters in analysis of fluid flow over airfoils is to find the separation point location. The lift coefficient is one of the most important parameters in the design of wind turbine airfoils, and it is significantly affected by vortex generation and recirculation flows over the suction surface of a wind turbine blade. Based on the spectral-hp element method, the mesh size can be refined by increasing the polynomial order (P) of the elements. The lift coefficient over the surface of the stationary NACA-0012 airfoil is computed at Re=135,000 and AoA=10° to select the find the suitable P-order for further simulations over stationary and oscillating turbine airfoils. The lift coefficients for different P-orders are provided in Table 2. It is observed that by raising P from 3 to 5, the deviation is significant (44.6%), and it is reduced by increasing P up to 11. It can be seen that the deviation for the C_L between P=9 and 11 is less than 1%. Therefore, the aerodynamic characteristics will be reliable and accurate enough at P=9, which is used for the next simulations. The same method is applied for both stationary and oscillating airfoils at different Reynolds numbers to ensure the precision of the DNS results.

Table 2. GRID INDEPENDENCE STUDY FOR DIFFERENT P-ORDERS AT RE=135,000 and AoA=10°.

Polynomial order	C_L	Deviation
P=3	0.439	-
P=5	0.635	44.6%
P=7	0.763	20.2%
P=9	0.812	6.4%
P=11	0.815	0.37%

4. RESULTS AND DISCUSSION

4.1. Validation

The numerical results for the lift coefficients over the surface of the NACA-0012 at different AoAs are validated with previous experimental and numerical data available in literature [42, 43] at Re=1.35×10^5. It can be seen that the present DNS results are in excellent agreement with the experimental results of Lee and Gerontakos [42]. The comparison showed that the present study, can precisely predict the stall over the stationary airfoil. However, there is a small deviation between the present unsteady analysis and 2D results of Shen et al. [43] in the stall region. The main reason for these small deviations is that they used a simplified two-dimensional model for their computations, while a high-fidelity DNS method is employed in the current study and agrees well with the realistic experimental measurements.

The pressure coefficient over the suction side and pressure side of a NACA-0012 airfoil is compared and validated with the experimental results of Rinoie and Takemura [44] in Figure 6. The validations are conducted at Re=1.3×10^5 without considering the flap-wise oscillations. It can be seen that the present DNS results are in excellent agreement with the experiments. The small deviations between the experiments and the numerical results are due to the laminar separation bubble formation on the suction surface of the blade which is slightly larger in the numerical analysis.

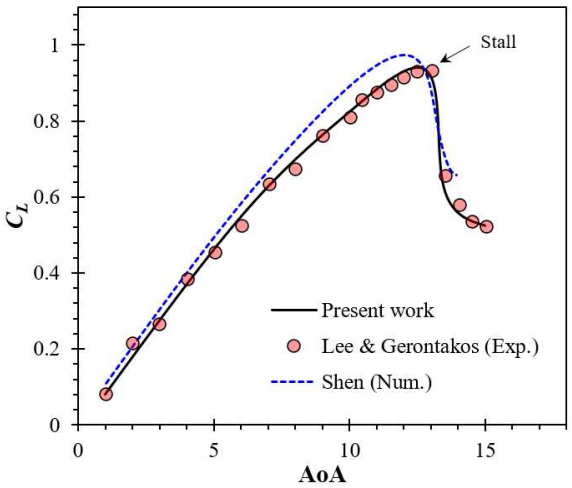

FIGURE 5: VALIDATION OF LIFT COEFFICIENT OVER STATIONARY AIRFOIL AT RE=1.3×10^5.

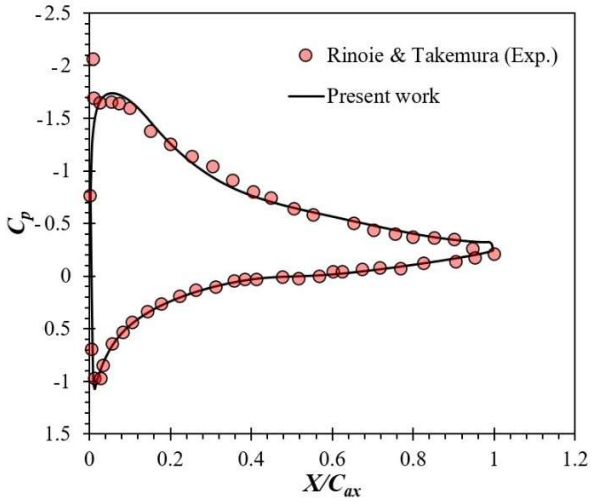

FIGURE 6: VALIDATION OF THE PRESSURE COEFFICIENT OVER STATIONARY AIRFOIL AT α=0º.

4.2. Aerodynamic characteristics

Figure 7 shows effects of angle of attack on instantaneous velocity contours and flow streamlines over stationary NACA-0012 wind turbine airfoil at two different Reynolds numbers of 5×10^4 and 1.35×10^5. It can be seen that the disturbance and recirculating flows become larger by raising the angle of attack, specially at lower Reynolds numbers. The results show that the flow separation occurs much faster at AoA of 20º, which has significant influence on stall, and reduction in the lift coefficient. The laminar separation bubbles (LSB) are formed on the suction side of the airfoils in the boundary-layer separated region. It can be seen that the size of LSB is larger at higher angle of attacks. Moreover, the separated shear layer and vortex shedding away from the TE of the airfoils is detected. At Re=5×10^4, with AoA=0º, Von-Karman vortex shedding is detected near the trailing edge of the blade and the flow remains attached on the pressure surface of the turbine blade. It is observed that in the stall regions (AoA>12º) the flow disturbance and vortex generation at different inflow speeds are nearly identical. Physically speaking, the separated flow region is mostly affected by the AoA, and flow separation occurs near the leading edge of the wind turbine airfoil at AoA=20º.

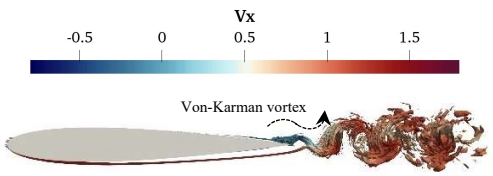

(a) Re=5×10^4, AoA=0º

(b) Re=1.35×10^5, AoA=0º

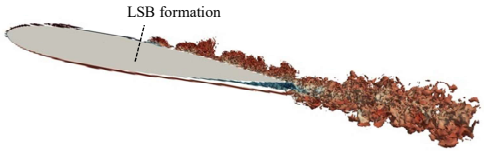

(c) Re=5×10^4, AoA=12º

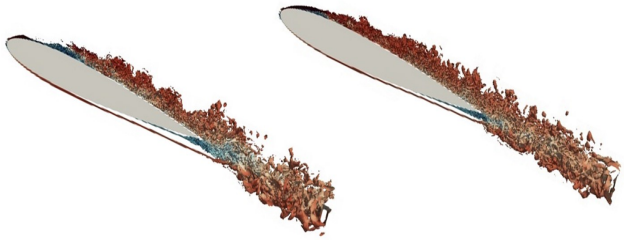

(d) Re=5×10^4, AoA=20º (e) Re=1.35×10^5, AoA=20º

FIGURE 7: VORTICITY CONTOURS OVER WIND TURBINE AIRFOIL AT DIFFERENT ANGLE OF ATTACKS AND REYNOLDS NUMBERS.

Figure 8 depicts the instantaneous vorticity contours over both stationary and oscillating airfoil at Re=50,000. The results show that the oscillations have noticeable impact on the size of vorticities in the separated region. At the same angle of attack, the vorticity generation become much larger over the oscillating blade, and the flow separation occurs faster. Therefore, the lift coefficient is expected to reduce due to the flap-wise vibrations. At AoA=0º, the separated shear layer rolling up, and shedding from the trailing edge (TE) is observed. But the blades vibrations impose extra flow disturbance on the suction side of the aerofoil before detachment from the TE. Therefore, it enhances perturbations in the wake region causing in additional velocity and pressure fluctuations and greater vorticities in the downstream area in comparison with the non-oscillating airfoil. Some small rolling up of the Kelvin–Helmholtz (KH) vorticities, are detected on both the pressure side and suction side of the WT airfoil close to the trailing edge, which shed from the trailing edge. It can be seen that the oscillations have influence on vortex generation on the pressure side of the blade. At both AoAs of 0 and 20 degrees, the flow separation occurs much faster on the suction side of the blade. However, the air velocity is higher near the leading edge of the blade at α=20º, which is due to the strong vortex generation and flow disturbance in the separation region.

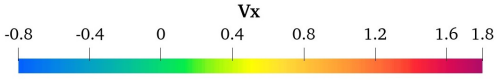

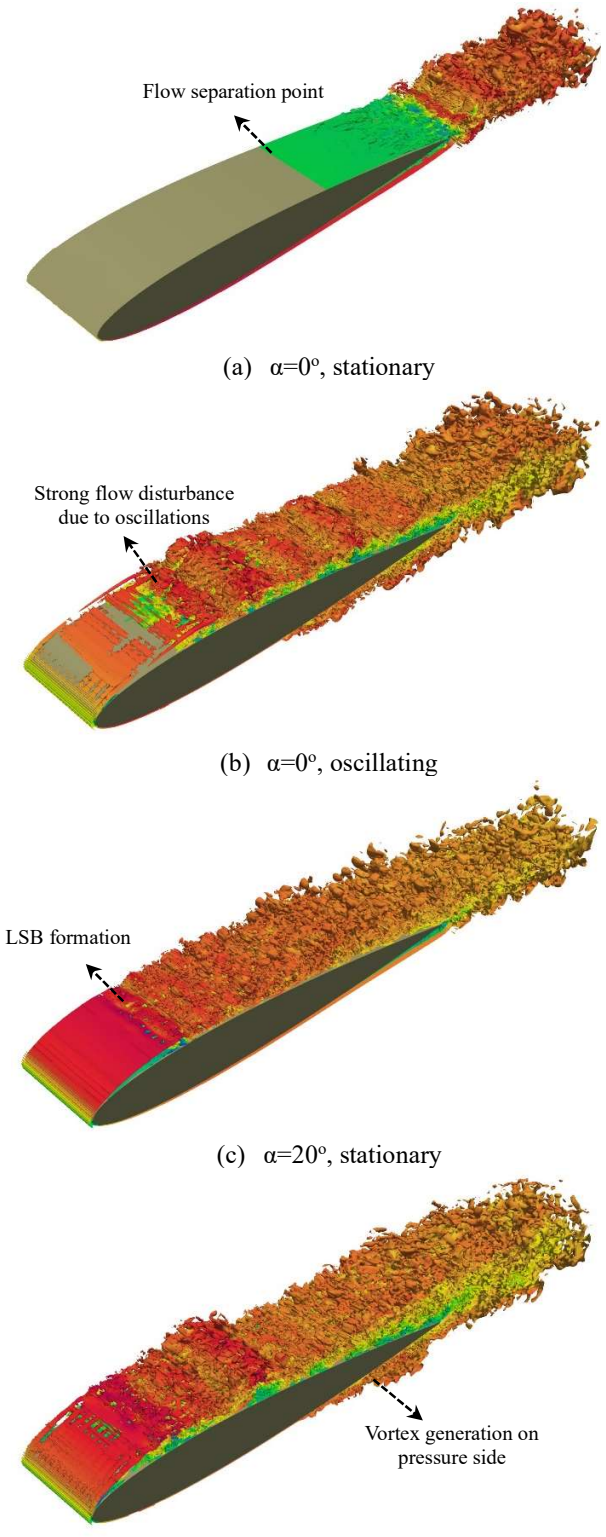

(a) α=0°, stationary

(b) α=0°, oscillating

(c) α=20°, stationary

(d) α=20°, oscillating

FIGURE 8: ISOSURFACE CONTOURS OF AXIAL VELOCITY OVER STATIONERY AND OSCILLATING BLADES AT RE=1.35×10^5.

The pressure coefficient varies on the surface of the wind turbine blade during a pitch-wise oscillating period. The pressure values are higher on the pressure side of the airfoil compared to the suction side. Moreover, the pressure fluctuations become noticeable in the separated flow regions, and they add additional flow disturbance in the wake region. Therefore, to better discuss the effects of vibrations on air flow pressure during a vibration period, the pressure distribution can be expressed by unsteady pressure coefficient (C_{p1}) and pressure phase angle (φ). These parameters can describe the flow instabilities and vortex generation over the surface of the oscillating blades. The time-averaged values of the pressure coefficient (C_p) become similar for both stationary and oscillating wind turbine blade.

To perform further post-processing, the Navier-Stokes equation can be written in the vector form of the conservative parameters (Q), and lumped residuals and source terms (R), as $\frac{\partial Q}{\partial t} = R(Q)$. Basically, Fourier series are used to find the time averaged and fluctuation parts and only the fundamental harmonic is considered here. The time dependent values are obtain using the DNS. According to the study of Rahmati et al. [45, 46], the fluid flow parameters over the vibrating blade with a vibration frequency of ($\omega = 2\pi f$), can be written as:

$$Q = \tilde{Q} + A_Q \sin(\omega t) + B_Q \cos(\omega t) \quad (9)$$

Where $\tilde{Q}$, A_Q and B_Q are the Fourier coefficients of the variable parameters. By replacing the above equation in $\frac{\partial Q}{\partial t} = R(Q)$, the equation can be expressed as:

$$\omega\left(A_Q \cos(\omega t) - B_Q \sin(\omega t)\right) = R'(Q) \quad (10)$$

According to this equation, the conservative parameters at three different vibration phases ($\omega t = 0, \pm\pi/2$) can be expressed as:

$$Q_0 = \tilde{Q} + B_Q \text{ at } \omega t = 0$$
$$Q_0 = \tilde{Q} + A_Q \text{ at } \omega t = \pi/2 \quad (11, \text{a-c})$$
$$Q_0 = \tilde{Q} - A_Q \text{ at } \omega t = -\pi/2$$

By using these three algebraic equations, the unknown parameters $\tilde{Q}$, A_Q and B_Q can be evaluated.

During a vibration period, the pressure can be expressed as $P = P_{Avrg} + P_A \sin(\omega t) + P_B \cos(\omega t)$, where P_{Avrg} is the average pressure used for the computation of pressure coefficient (C_p). The unsteady pressure coefficient (C_{p1}) and pressure phase angle (ϕ), can be computed by $C_{p1} = \sqrt{P_A^2 + P_B^2}$, and $\phi = \tan^{-1}(\frac{P_A}{P_B})$. The variations of the unsteady pressure coefficient and pressure phase angle over the surface of the oscillating wind turbine NACA-0012 airfoil are shown in Figure 9. At higher angle of attack of 20°, the unsteady pressure coefficient is higher on the surface of the blade in the X direction compared to the lower AoA of 0°. After flow separation occurrence, the pressure coefficient significantly decreased due to the vortex generation and recirculating flows in the separated shear layer. It can be seen that the unsteady pressure fluctuations are smaller at the zero angle of attack. As discussed earlier, flow detachment and reattachment on the surface of the oscillating blade with higher angle of attacks, is the main reason for the pressure fluctuations in stall conditions. Besides, these fluctuations cause noticeable

decrement in the lift coefficient on the surface of the turbine blades.

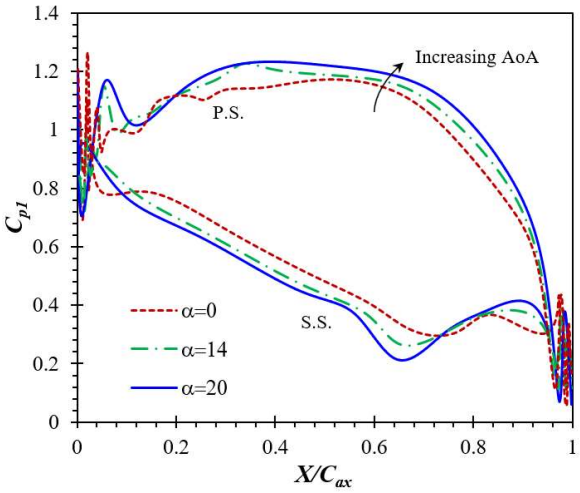

FIGURE 9: UNSTEADY PRESSURE COEFFICIENT OVER OSCILLATING WIND TURBINE BLADE FOR DIFFERENT ANGLE OF ATTACKES AT RE=1.35×10^5.

Figure 10 shows the energy spectrum of both stationary and pitch-wise oscillating airfoil. The results show that for both cases, the energy spectrum falls below the −5/3-slope line, which corresponds to the characteristic slope of the turbulent flow over the blade. It is observed that the results are converged for both cases and due to the numerical instabilities, the peak occurs at 6.82 Hz on the oscillating airfoil. The PSD profiles are plotted for the P-order of 11.

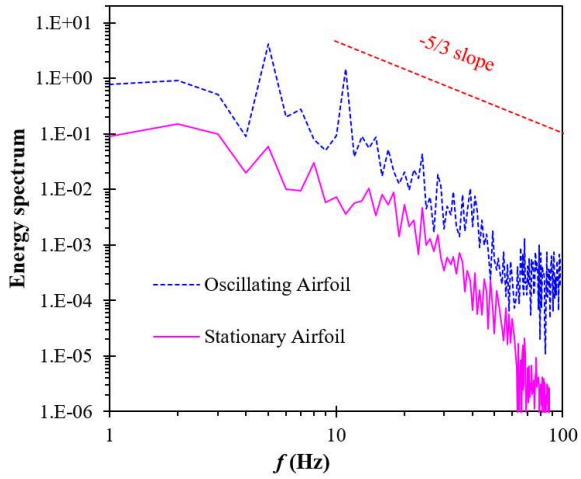

FIGURE 10: ENERGY SPCTRAL DENSITY OVER STATIONERY AND OSCILLATING TURBINE AIRFOIL AT RE=1.35×10^5.

5. CONCLUSION

In this study, direct numerical simulations are employed for the first time to investigate the instantaneous vorticities and flow separation over NACA-0012 airfoil by considering the pitch-wise oscillations. The simulations were performed with the spectral-hp element method which is a powerful method for high-fidelity aerodynamic analysis. All realistic flow conditions over the wind turbine airfoil were considered, and the simulations were performed at two different Reynolds numbers of Re=5×10^4, and 1.35×10^5 at different angles of attack.

The simulations revealed that the proposed model is more accurate compared to previous numerical models, which were mostly focused on two-dimensional airfoil sections. The results show that the flow separation occurs much faster at AoA of 20^o, which has noticeable influence on stall occurrence, which reduces the favorable lift significantly. The laminar separation bubbles (LSB) are generated on the suction side of the airfoils in the boundary-layer separated region. At Re=5×10^4, with AoA=0^o, Von-Karman vortex shedding is detected near the trailing edge of the blade and the flow remains attached on the pressure surface of the turbine blade. It is observed that in the stall regions, the flow disturbance and vortex generation at different inflow speeds are nearly identical. Physically speaking, the separated flow region is mainly impacted by the inflow direction, and flow separation occurs near the leading edge of the airfoil at AoA=20^o.

The effects of angle of attack on the unsteady pressure coefficient on both the suction and pressure sides of the blade are also investigated. The pitch-wise oscillations add additional flow perturbations on the suction side of the airfoil before detachment from the TE. Thus, it enhances perturbations in the wake region causing in additional velocity and pressure fluctuations and greater vorticities in the downstream area in comparison with the non-oscillating airfoil. Some small rolling up of the Kelvin–Helmholtz (KH) vorticities, are detected on both the pressure side and suction side of the WT airfoil close to the trailing edge, which shed from the trailing edge.

Further research must be conducted in future to investigate the effects of advanced hybrid wake control techniques on performance improvement of complex wind farm layouts by considering all realistic flow conditions over the turbine blades.

REFERENCES

[1] J. Dai, X. Yang, W. Hu, L. Wen, Y. Tan, Effect investigation of yaw on wind turbine performance based on SCADA data, Energy, 149 (2018) 684-696.

[2] P. Pourazarm, Y. Modarres-Sadeghi, M.A. Lackner, Flow-induced instability of wind turbine blades, 32nd ASME Wind Energy Symposium, 2014, pp. 1219.

[3] F. Khalili, P. Majumdar, M. Zeyghami, Far-field noise prediction of wind turbines at different receivers and wind speeds: A computational study, ASME International Mechanical Engineering Congress and Exposition, American Society of Mechanical Engineers, 2015, pp. V07BT09A051.

[4] M. Nakhchi, S.W. Naung, M. Rahmati, High-resolution direct numerical simulations of flow structure and aerodynamic

performance of wind turbine airfoil at wide range of Reynolds numbers, Energy, 225 (2021) 120261.
[5] S.W. Naung, M.E. Nakhchi, M. Rahmati, An Experimental and Numerical Study on the Aerodynamic Performance of Vibrating Wind Turbine Blade with Frequency- Domain Method, Journal of Applied and Computational Mechanics, DOI (2021).
[6] S.W. Naung, M.E. Nakhchi, M. Rahmati, High-fidelity CFD simulations of two wind turbines in arrays using nonlinear frequency domain solution method, Renewable Energy, 174 (2021) 984-1005.
[7] K. Koca, M.S. Genç, H.H. Açıkel, M. Çağdaş, T.M. Bodur, Identification of flow phenomena over NACA 4412 wind turbine airfoil at low Reynolds numbers and role of laminar separation bubble on flow evolution, Energy, 144 (2018) 750-764.
[8] T. Zhang, Z. Wang, W. Huang, D. Ingham, L. Ma, M. Pourkashanian, A numerical study on choosing the best configuration of the blade for vertical axis wind turbines, Journal of Wind Engineering and Industrial Aerodynamics, 201 (2020) 104162.
[9] A. Saleem, M.-H. Kim, Effect of rotor tip clearance on the aerodynamic performance of an aerofoil-based ducted wind turbine, Energy Conversion and Management, 201 (2019) 112186.
[10] H.H. Açıkel, M.S. Genc, Control of laminar separation bubble over wind turbine airfoil using partial flexibility on suction surface, Energy, 165 (2018) 176-190.
[11] R. Wahidi, W. Lai, J.P. Hubner, A. Lang, Volumetric three-component velocimetry and PIV measurements of Laminar Separation Bubbles on a NACA4412 Airfoil, 16th Int. Symp of applications of laser techniques of fluid mechanics, 2012.
[12] A. Arabgolarcheh, E. Benini, M. Anbarsooz, Development of an Actuator Line Model for Simulation of Floating Offshore Wind Turbines, ASME Power Conference, American Society of Mechanical Engineers, 2021, pp. V001T009A001.
[13] M. O'meara, T.J. Mueller, Laminar separation bubble characteristics on an airfoil at low Reynolds numbers, AIAA journal, 25 (1987) 1033-1041.
[14] M. Alam, N.D. Sandham, Direct numerical simulation of'short'laminar separation bubbles with turbulent reattachment, Journal of Fluid Mechanics, 410 (2000) 1-28.
[15] T.-t. Zhang, M. Elsakka, W. Huang, Z.-g. Wang, D.B. Ingham, L. Ma, M. Pourkashanian, Winglet design for vertical axis wind turbines based on a design of experiment and CFD approach, Energy Conversion and Management, 195 (2019) 712-726.
[16] G. Karniadakis, S. Sherwin, Spectral/hp element methods for computational fluid dynamics, Oxford University Press2013.
[17] S.J. Sherwin, M. Ainsworth, Unsteady Navier–Stokes solvers using hybrid spectral/hp element methods, Applied Numerical Mathematics, 33 (2000) 357-363.
[18] D. Moxey, C.D. Cantwell, Y. Bao, A. Cassinelli, G. Castiglioni, S. Chun, E. Juda, E. Kazemi, K. Lackhove, J. Marcon, Nektar++: Enhancing the capability and application of high-fidelity spectral/hp element methods, Computer Physics Communications, 249 (2020) 107110.
[19] A. Cassinelli, P. Adami, F. Montomoli, S.J. Sherwin, On the effect of wake passing on a low pressure turbine cascade using spectral/\textit {hp} element methods, Bulletin of the American Physical Society, 64 (2019).
[20] I.S. Hwang, S.Y. Min, I.O. Jeong, Y.H. Lee, S.J. Kim, Efficiency improvement of a new vertical axis wind turbine by individual active control of blade motion, Smart Structures and Materials 2006: Smart Structures and Integrated Systems, International Society for Optics and Photonics, 2006, pp. 617311.
[21] J. Lei, J. Zhang, J. Niu, Effect of active oscillation of local surface on the performance of low Reynolds number airfoil, Aerospace Science and Technology, 99 (2020) 105774.
[22] D. Munday, J. Jacob, Active control of separation on a wing with oscillating camber, Journal of aircraft, 39 (2002) 187-189.
[23] V. Katam, R. LeBeau, J. Jacob, Simulation of separation control on a morphing wing with conformal camber, 35th AIAA Fluid Dynamics Conference and Exhibit, 2005, pp. 4880.
[24] L.W. Carr, K.W. McAlister, W.J. McCroskey, Analysis of the development of dynamic stall based on oscillating airfoil experiments, DOI (1977).
[25] W.J. McCroskey, K.W. McAlister, L.W. Carr, S. Pucci, An Experimental Study of Dynamic Stall on Advanced Airfoil Sections. Volume 1. Summary of the Experiment, NATIONAL AERONUATICS AND SPACE ADMINISTRATION MOFFETT FIELD CA AMES RESEARCH …, 1982.
[26] R. Piziali, 2-D and 3-D oscillating wing aerodynamics for a range of angles of attack including stall, DOI (1994).
[27] J. Ekaterinaris, F. Menter, Computation of oscillating airfoil flows with one-and two-equation turbulence models, AIAA journal, 32 (1994) 2359-2365.
[28] M. Raffel, J. Kompenhans, P. Wernert, Investigation of the unsteady flow velocity field above an airfoil pitching under deep dynamic stall conditions, Experiments in Fluids, 19 (1995) 103-111.
[29] R. Ramsay, M. Hoffman, G. Gregorek, Effects of grit roughness and pitch oscillations on the S809 airfoil, National Renewable Energy Lab., Golden, CO (United States), 1995.
[30] G.N. Barakos, D. Drikakis, Unsteady separated flows over manoeuvring lifting surfaces, Philosophical Transactions of the Royal Society of London. Series A: Mathematical, Physical and Engineering Sciences, 358 (2000) 3279-3291.
[31] T. Lee, P. Gerontakos, Investigation of flow over an oscillating airfoil, Journal of Fluid Mechanics, 512 (2004) 313.
[32] X. Amandolese, E. Szechenyi, Experimental study of the effect of turbulence on a section model blade oscillating in stall, Wind Energy: An International Journal for Progress and Applications in Wind Power Conversion Technology, 7 (2004) 267-282.
[33] S. Wang, D.B. Ingham, L. Ma, M. Pourkashanian, Z. Tao, Numerical investigations on dynamic stall of low Reynolds number flow around oscillating airfoils, Computers & fluids, 39 (2010) 1529-1541.
[34] Y. Kim, Z.-T. Xie, Modelling the effect of freestream turbulence on dynamic stall of wind turbine blades, Computers & Fluids, 129 (2016) 53-66.

[35] K. Gharali, D.A. Johnson, Dynamic stall simulation of a pitching airfoil under unsteady freestream velocity, Journal of Fluids and Structures, 42 (2013) 228-244.
[36] C. Zhu, Y. Qiu, T. Wang, Dynamic stall of the wind turbine airfoil and blade undergoing pitch oscillations: A comparative study, Energy, 222 (2021) 120004.
[37] H. Jokar, M. Mahzoon, R. Vatankhah, Dynamic modeling and free vibration analysis of horizontal axis wind turbine blades in the flap-wise direction, Renewable Energy, 146 (2020) 1818-1832.
[38] S.W. Naung, M. Rahmati, H. Farokhi, Nonlinear frequency domain solution method for aerodynamic and aeromechanical analysis of wind turbines, Renewable Energy, 167 (2021) 66-81.
[39] C.D. Cantwell, D. Moxey, A. Comerford, A. Bolis, G. Rocco, G. Mengaldo, D. De Grazia, S. Yakovlev, J.-E. Lombard, D. Ekelschot, Nektar++: An open-source spectral/hp element framework, Computer physics communications, 192 (2015) 205-219.
[40] J.-L. Guermond, J. Shen, Velocity-correction projection methods for incompressible flows, SIAM Journal on Numerical Analysis, 41 (2003) 112-134.
[41] S. Dong, G.E. Karniadakis, C. Chryssostomidis, A robust and accurate outflow boundary condition for incompressible flow simulations on severely-truncated unbounded domains, Journal of Computational Physics, 261 (2014) 83-105.
[42] T. Lee, P. Gerontakos, Investigation of flow over an oscillating airfoil, Journal of Fluid Mechanics, 512 (2004) 313-341.
[43] X. Shen, E. Avital, M.A. Rezaienia, G. Paul, T. Korakianitis, Computational methods for investigation of surface curvature effects on airfoil boundary layer behavior, Journal of Algorithms & Computational Technology, 11 (2017) 68-82.
[44] K. Rinoie, N. Takemura, Oscillating behaviour of laminar separation bubble formed on an aerofoil near stall, The aeronautical journal, 108 (2004) 153-163.
[45] M. Rahmati, L. He, D. Wang, Y. Li, R. Wells, S. Krishnababu, Nonlinear time and frequency domain methods for multirow aeromechanical analysis, Journal of Turbomachinery, 136 (2014) 041010.
[46] M. Nakhchi, S.W. Naung, M. Rahmati, Influence of blade vibrations on aerodynamic performance of axial compressor in gas turbine: Direct numerical simulation, Energy, 242 (2022) 122988.